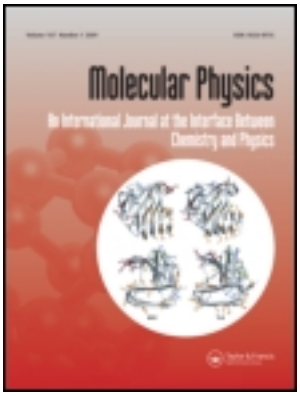

Molecular Physics: An International Journal at the Interface Between Chemistry and Physics
Publication details, including instructions for authors and subscription information:
http://www.tandfonline.com/loi/tmph20

On the Curie points and high temperature susceptibilities of Heisenberg model ferromagnetics

G.S. Rushbrooke [a] & P.J. Wood [a]
[a] Physics Department, King's College, University of Durham, Newcastle upon Tyne

Version of record first published: 23 Aug 2006.

To cite this article: G.S. Rushbrooke & P.J. Wood (1958): On the Curie points and high temperature susceptibilities of Heisenberg model ferromagnetics, Molecular Physics: An International Journal at the Interface Between Chemistry and Physics, 1:3, 257-283

To link to this article: http://dx.doi.org/10.1080/00268975800100321

On the Curie points and high temperature susceptibilities of Heisenberg model ferromagnetics

by G. S. RUSHBROOKE and P. J. WOOD
Physics Department, King's College, Newcastle upon Tyne,
University of Durham

(*Received* 14 *May* 1958)

The first six coefficients in the expansion of the susceptibility χ, and its inverse, χ^{-1}, in ascending powers of the reciprocal temperature, have been determined for the Heisenberg model of a ferromagnetic, for any spin value, S, and any lattice. The first five coefficients appropriate to the magnetic specific heat, C, have also been found. For the body-centred and face-centred cubic lattices, the χ and C coefficients are tabulated for half-integral S from $\frac{1}{2}$ to 3.

From these coefficients estimates have been made of the reduced Curie temperatures, $\theta_c = kT_c/J$. It is found that for the simple, body-centred and face-centred cubic lattices the formula

$$\theta_c = \tfrac{5}{96}(z-1)(11X-1)$$

reproduces the estimated Curie temperatures fairly accurately. Here $X = S(S+1)$ and z is the lattice coordination-number.

It is found that, suitably scaled, the theoretical curves for inverse susceptibility against temperature above the Curie point are rather insensitive to the spin value and to the precise lattice structure. The ratio of their initial to their final gradients is approximately 0·3. A comparison is made with the experimental values of χ^{-1} for both iron and nickel. If iron is represented by the Heisenberg model with $S=1$, then the observed Curie temperature corresponds to a J value of $1{\cdot}19\times10^{-2}$ ev.

Brief consideration is given to the use of the tabulated coefficients for antiferromagnetic problems.

1. Introduction

Our purpose in this paper is to present expressions for the leading coefficients in the expansion in inverse powers of the temperature, of the magnetic susceptibility, χ, for the Heisenberg model of a ferromagnetic substance. We consider the generalized Heisenberg model for arbitrary spin, S, and the work is consequently based on the Hamiltonian, $\mathscr{H}$, given by

$$\mathscr{H} = -2J \sum_{\langle i,j \rangle} \mathbf{S}^{(i)} . \mathbf{S}^{(j)} - g\beta H \sum_i S_3^{(i)}. \qquad (1)$$

Equation (1) relates to a lattice of N sites, labelled $1, 2, \ldots i \ldots j \ldots N$. $\mathbf{S}^{(i)}$ denotes a spin variable (with components S_1, S_2, S_3) located on the ith site, and the exchange energies, J, are invoked between neighbouring sites only (pairs of neighbouring sites being denoted by $\langle i,j \rangle$). The z-axis is taken in the direction of the external magnetic field, H: β denotes the Bohr magneton and g the gyromagnetic ratio.

As is well known, for any matrix representation of $\mathscr{H}$ the partition function, Z, for the system is given by

$$Z = \text{trace}\,[\exp(-\mathscr{H}/\boldsymbol{k}T)] \tag{2}$$

and then

$$\chi = \frac{\partial^2}{\partial H^2}(\boldsymbol{k}T \ln Z). \tag{3}$$

At low temperatures the problem is usually treated by spin-wave theory. We are here concerned, however, with high temperatures, above the Curie point, and proceed by expanding Z, and thence χ, in powers of $1/\boldsymbol{k}T$. It is convenient to work in terms of the reduced temperature θ, given by $\boldsymbol{k}T/J$, and the reduced susceptibility $\bar{\chi}$, given by $J\chi/Ng^2\beta^2$, and in terms of these variables to write

$$\bar{\chi}\theta = \tfrac{1}{3}S(S+1)\sum_{n=0}^{\infty}\frac{a_n}{\theta^n}, \tag{4}$$

and

$$\frac{1}{\bar{\chi}\theta} = \frac{3}{S(S+1)}\sum_{n=0}^{\infty}\frac{b_n}{\theta^n}. \tag{5}$$

We shall consider only the zero-field susceptibility: thus our immediate purpose is to derive expressions for the coefficients $a_1, a_2 \ldots a_6$, and $b_1, b_2 \ldots b_6$, in equations (4) and (5), in the limit as $H \to 0$. The coefficients a_0 and b_0 are each unity.

There has, of course, been much earlier work on this problem: in particular that of Opechowski [1, 2] and Zehler [3] for the special case $S = \frac{1}{2}$ and that of Brown and Luttinger [4] and Brown [5] for general spin S: but except for Brown (see below) these authors did not go beyond the fourth coefficients a_4 or b_4. In 1955 the present authors gave general expressions, suitable for any lattice, for the first five coefficients in the case $S = \frac{1}{2}$ [6], and shortly afterwards Domb and Sykes [7] produced the sixth coefficients for this case. The interest in getting as many coefficients as possible lies in the use made of the series (4) or (5) for estimating the Curie temperature of the model, and we return to the Curie temperature problem below, after first finding the coefficients.

For this general problem we have already presented elsewhere [8] a brief summary of results as far as a_5: and we noted disagreement with Brown [5]. Now that the sixth coefficients have been found (and we have no intention of going further) it seems appropriate to present the results in a self-contained paper, including an indication of the mathematical techniques employed, and to use the coefficients to estimate as accurately as possible the corresponding Curie temperatures. It is, of course, true that the Hamiltonian (1) is perhaps more applicable physically to antiferromagnetic problems, with J negative, than to ferromagnetic problems with J positive. While this does not diminish the theoretical interest of the predicted Curie temperatures it is perhaps pertinent to observe that the corresponding series for the antiferromagnetic problem are simply obtained from (4) and (5) by replacing a_n and b_n by $(-1)^n a_n$ and $(-1)^n b_n$ respectively. In the definitions of θ and $\bar{\chi}$, J has, of course, to be replaced by $|J|$ (see Danielian and Stevens [9] and § 10 below).

We shall also give expressions for coefficients pertaining to the magnetic specific heat above the Curie temperature: but in most cases the expansion of

this quantity appears to be poorly convergent. Again these coefficients, c_n, must be replaced by $(-1)^n c_n$ in the antiferromagnetic problem.

2. Expressions for a_n and c_n

If we introduce the convenient notations

$$\sum_{\langle i,j\rangle} \mathbf{S}^{(i)}.\mathbf{S}^{(j)} = P, \qquad \sum_i S_3^{(i)} = Q, \qquad g\beta H/2J = \alpha$$

and, for any operator A, $\langle A\rangle = \text{trace } A/(2S+1)^N$, then equation (2) reads

$$Z = (2S+1)^N \sum_{r=0}^{\infty} \frac{2^r}{r!}\frac{\mu_r}{\theta^r} \tag{6}$$

where $\mu_r = \langle (P+\alpha Q)^r\rangle$. Now $\mu_0 = 1$, since when $r=0$ we require $\langle I\rangle$ where I represents the direct product of N spin matrices each with trace $2S+1$. Thus (6) gives

$$\begin{aligned} \ln Z &= N\ln(2S+1) + \ln\left[1 + \sum_{r=1}^{\infty} \frac{2^r\mu_r}{r!\,\theta^r}\right] \\ &= N\ln(2S+1) + \sum_{r=1}^{\infty} \frac{2^r\lambda_r}{r!\,\theta^r} \end{aligned} \tag{7}$$

where, in the language of statistics, the coefficients λ_r are the cumulants corresponding to the moments μ_r. More simply, they are in fact those parts of the moments which are directly proportional to N: for, as is dimensionally necessary, λ_r is found to be proportional to N and

$$\mu_r = \lambda_r + \text{terms involving } N^2, N^3 \text{ etc.}, \tag{8}$$

these latter terms cancelling when we transform from moments to cumulants.

Expanding μ_r (and thence λ_r) in powers of α, we may write

$$\begin{aligned} \mu_r &= \mu_r^{(0)} + \alpha\mu_r^{(1)} + \alpha^2\mu_r^{(2)} + \ldots \\ \lambda_r &= \lambda_r^{(0)} + \alpha\lambda_r^{(1)} + \alpha^2\lambda_r^{(2)} + \ldots \end{aligned} \tag{9}$$

and, from (8), $\lambda_r^{(l)}$ is that part of $\mu_r^{(l)}$ which is directly proportional to N. With these preliminaries we can turn to the calculation of the susceptibility χ and magnetic specific heat C: and in both cases we shall be interested solely in their values in zero external field H, i.e. when α is put equal to zero at the end of the calculation.

First, the susceptibility χ. From (3), (7) and (9)

$$\bar{\chi}\theta = \frac{1}{N}\sum_{r=1}^{\infty} \frac{2^{r-1}}{r!}\frac{\lambda_r^{(2)}}{\theta^{r-2}}. \tag{10}$$

But $\lambda_1^{(2)} = 0$ and, since $\mu_1 = 0$, $\lambda_2^{(2)} = \mu_2^{(2)} = \langle Q^2\rangle = \frac{1}{3}S(S+1)N$. Thus $\bar{\chi}\theta$ can be written as in (4) with $a_0 = 1$ and

$$a_n = \frac{3}{S(S+1)} \cdot \frac{2^{n+1}}{(n+2)!}\frac{\lambda_{n+2}^{(2)}}{N}. \tag{11}$$

Since P and Q commute, $(P+\alpha Q)^r = P^r + rP^{r-1}Q\alpha + \frac{1}{2}r(r-1)P^{r-2}Q^2\alpha^2 + \ldots$, and consequently (11) becomes

$$a_n = \frac{3}{S(S+1)} \cdot \frac{2^n}{n!}\{\text{coefficient of } N \text{ in } \langle P^nQ^2\rangle\}, \tag{12}$$

which is the basic formula from which we calculate the coefficients a_n in the expansion (4).

Secondly, the magnetic specific heat, C, is given by

$$C = \frac{\partial}{\partial T}\left[\boldsymbol{k}T^2 \frac{\partial}{\partial T} \ln Z\right], \tag{13}$$

with $H=0$. Consequently, from (7) and (9)

$$C = \frac{4\boldsymbol{k}}{\theta^2}\lambda_2^{(0)}\left[1+\sum_{n=1}^{\infty}\frac{c_n}{\theta^n}\right], \qquad \text{where} \quad c_n = \frac{2^n}{n!}\cdot\frac{\lambda_{n+2}^{(0)}}{\lambda_2^{(0)}}.$$

But $\lambda_2^{(0)}=\mu_2^{(0)}=\langle P^2\rangle$ and, by an elementary application of the methods outlined below, we find $\langle P^2\rangle = \frac{1}{6}Nz S^2(S+1)^2$, where z denotes the coordination-number of the lattice. Thus

$$\frac{C}{N\boldsymbol{k}} = \frac{c}{\theta^2}\left[1+\sum_{n=1}^{\infty}\frac{c_n}{\theta^n}\right] \tag{14}$$

where

$$c = \tfrac{2}{3}zS^2(S+1)^2 \tag{15}$$

and

$$c_n = \frac{3\,.\,2^{n-1}}{zS^2(S+1)^2}\cdot\frac{1}{n!}\{\text{coefficient of } N \text{ in } \langle P^{n+2}\rangle\}. \tag{16}$$

To find a_n and c_n, therefore, we require to calculate the parts linearly dependent on N in $\langle P^n Q^2\rangle$ and $\langle P^{n+2}\rangle$; and we have proceeded as far as $\langle P^6Q^2\rangle$ and $\langle P^7\rangle$, i.e. a_6 and c_5. As we shall see, the calculation of c_{n-1} is closely related to that of a_n and does not entail much extra work.

3. Calculation of $\langle P^n\rangle$

It is convenient at the outset to abbreviate $S(S+1)$ and $2S+1$ to X and Y, respectively. Then $\langle P^n\rangle = Y^{-N}\,\text{trace}\,(\sum \mathbf{S}^{(i)}\,.\,\mathbf{S}^{(j)})^n$, and any term in the expansion of P^n can be represented by a set of n lines joining neighbouring pairs of sites on the lattice. Any such set of n lines will be said to form a diagram of order n: but in classifying the possible diagrams we do not specify the particular lattice sites concerned, simply the topology of the connections. Thus, for $n=2$, $(\mathbf{S}^{(1)}\,.\,\mathbf{S}^{(2)})^2$ and $(\mathbf{S}^{(2)}\,.\,\mathbf{S}^{(3)})^2$ would each be said to be represented by the diagram ═══, while $(\mathbf{S}^{(1)}\,.\,\mathbf{S}^{(2)})(\mathbf{S}^{(2)}\,.\,\mathbf{S}^{(3)})$ would be represented by the diagram ·—·—· whatever the angle between the bonds (12) and (23). To find P^n, therefore, we have

(a) to enumerate all possible diagrams consisting of n lines,

(b) to calculate the traces of the products of spin variables corresponding to each diagram, and

(c) to specify the number of times that each diagram can occur, on the lattice of N distinct sites. The crux of the problem lies in (b): but we first comment briefly on (a) and (c).

Since the trace of any component of a single spin matrix $\mathbf{S}$ vanishes, in enumerating diagrams under (a) we may ignore all those which contain any point having only one line attached to it. The diagrams with which we are concerned, therefore, consist either of multiple lines or of combinations of closed circuits (which may themselves contain multiple lines). From these we may further discard all those which would separate into two parts on the removal of a single line, as, for example, 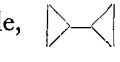 (see § 4 below). Even so, the number

of possible diagrams mounts rapidly with n. For $n=1, 2, \ldots 7$, we find 0, 1, 2, 5, 10, 31 and 71 diagrams, respectively. Some of these, of course, are composite diagrams, having two or more separate parts: for example, when $n=6$ a diagram can comprise two separate triangles. And for such a composite diagram, the trace is simply the product of the traces of the separate parts. The numbers of significant non-composite diagrams for $n=2, 3, \ldots 7$ are, in fact, 1, 2, 4, 8, 23 and 53 of these only comparatively few (0, 0, 0, 2, 2 and 3, respectively) were found subsequently to have zero trace.

In enumerating these diagrams no account is taken of specific lattice structure. Thus we include the possibility of triangles, pentagons, tetrahedra, etc., even though these cannot occur on a body-centred cubic lattice. The specific lattice characteristics are introduced at stage (c), through a set of lattice parameters (see below), of which the simplest is the coordination-number z, in terms of which the required occurrences can be expressed. The occurrence-factors for non-composite diagrams are directly proportional to N: but for a composite diagram of p parts we have terms in N^p, $N^{p-1} \ldots N$. The terms involving powers of N higher than the first cancel out in passing from moments to cumulants: as observed above. We have, of course, confirmed this in each case as a precautionary check on the calculations.

We turn now to (b), and must first observe that any particular diagram, even when its vertices are labelled (so that it corresponds to a precise set of lattice sites) still corresponds to a number of products of spin matrices which differ in the sequence of their factors. For example, the diagram

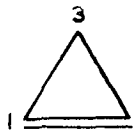

which arises in $\langle P^4 \rangle$ corresponds to the 12 terms

(12)(12)(13)(23)	(12)(13)(23)(12)	(13)(12)(23)(12)
(12)(12)(23)(13)	(12)(23)(13)(12)	(23)(12)(13)(12)
(12)(13)(12)(23)	(13)(12)(12)(23)	(13)(23)(12)(12)
(12)(23)(12)(13)	(23)(12)(12)(13)	(23)(13)(12)(12)

where (23), for instance, is short for $\mathbf{S}^{(2)} . \mathbf{S}^{(3)}$, i.e. $\sum_\alpha S_\alpha^{(2)} S_\alpha^{(3)}$, $\alpha = 1, 2, 3$. Thus the contribution to $\langle P^4 \rangle$ from this particular labelled diagram is Y^{-N} (sum of the traces of these 12 products). Now, in the $(2S+1)^N$-dimensional representation which we are using $S_\alpha^{(i)}$ is represented by the direct product $I \times I \times \ldots \times S_\alpha \times \ldots \times I$, where I denotes the $2S+1$ dimensional unit matrix and S_α, which occurs as the ith of N factors, denotes a $2S+1$ dimensional matrix representation of the spin component α. Consequently the contribution from this labelled diagram to $\langle P^4 \rangle$ may be written

$$Y^{-3} \operatorname{Tr} \sum_{(P)} (12)(12)(13)(23)$$

where $\sum_{(P)}$ denotes the 12 permutations of the subsequent brackets, and we now omit all mention of the sites 4, 5, ... N. Indeed, in general, for a diagram of n lines between s labelled sites, the contribution to $\langle P^n \rangle$ may be written

$$Y^{-s} \operatorname{Tr} \sum_{(P)} (\ )(\ ) \ldots (\ ) \qquad (17)$$

with n brackets to be permuted among themselves, and in computing these traces

we confine attention to a $(2S+1)^s$-dimensional representation of the spin matrices.

Returning to our particular example, since the trace of a matrix product is unaltered by cyclic permutation of the factors, we need compute specifically only the traces of the products

$$(12)(12)(13)(23), \qquad (12)(12)(23)(13) \quad \text{and} \quad (12)(13)(12)(23)$$

and of these the first two must be equal to due the symmetry of the diagram. To calculate them, we abbreviate S_α to α, adopt the summation convention, and write

$$\operatorname{Tr} \sum_{(P)} (12)(12)(13)(23) = \operatorname{Tr} \begin{bmatrix} & 1 & 2 & 3 \\ 8 & \alpha\beta\gamma & \alpha\beta\delta & \gamma\delta \\ +4 & \alpha\gamma\beta & \alpha\beta\delta & \gamma\delta \end{bmatrix}$$

where the columns headed 1, 2, 3 specify the sites on which the spin components are centred. Now the trace of the direct product of two matrices is the product of their traces, the trace of any single component of a spin matrix vanishes and, from the commutation rules, $\operatorname{Tr}\gamma\delta = 0$ unless $\gamma = \delta$. Moreover $\operatorname{Tr}\alpha\beta\gamma = 0$ unless α, β and γ are all different, and $\operatorname{Tr}\alpha\beta\gamma = -\operatorname{Tr}\alpha\gamma\beta$. Thus

$$\begin{aligned} \operatorname{Tr} \sum_{(P)} (12)(12)(13)(23) &= 4 \operatorname{Tr}(\alpha\beta\gamma) \operatorname{Tr}(\alpha\beta\gamma) \operatorname{Tr}(\gamma\gamma) \\ &= 24(\operatorname{Tr}(123))^2 \operatorname{Tr}(33) \\ &= 24(\tfrac{1}{6}iXY)^2(\tfrac{1}{3}XY) \qquad \text{(see Appendix I)} \\ &= -\tfrac{2}{9}X^3Y^3. \end{aligned}$$

We notice that the Y^3 cancels with the Y^{-3} above (this cancellation always occurs), and so find that the contribution from the labelled triangle with a double side to $\langle P^4 \rangle$ is $-\frac{2}{9}X^3$.

Every diagram has to be treated in essentially this way at stage (b), and the work is admittedly lengthy. Diagrams of n sides with no repeated lines correspond to $n!$ products and so, by the cyclic rule, to $(n-1)!$ separate traces. Symmetry, of the type illustrated above, may reduce this a little: even so, when $n=7$, some diagrams give rise to as many as 360 separate terms. A few typical diagrams, together with the numbers of terms to which they give rise, are given below:

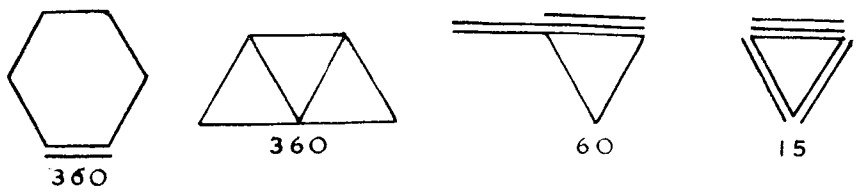

and we see that complexity is produced not only by the numbers of essentially different permutations but also by the number of lines meeting at a point, and thus the number of symbols α, β... at any one point in the trace calculation. This latter complexity appears unavoidable, and we list in Appendix I the basic traces required in the calculations. We have, however, found one theorem which sometimes reduces the work entailed by the more open diagrams, such as a seven-sided ring, or the first of those illustrated above, and we conclude this section with a statement of it, without proof.

Theorem I. If a non-composite diagram, D_l, of l lines, has somewhere three consecutive single lines $(ij)(jk)(km)$, the points j and k being not otherwise involved in the diagram, and if D_{l-1} is the diagram obtained by removing the centre one, (jk), of these lines, so making j and k coincide (the other parts of the diagram remaining unchanged), then, in an obvious notation,

$$\mathrm{Tr}\, D_l = \tfrac{1}{3}(1+\delta_{im})lXY\,\mathrm{Tr}\, D_{l-1}$$

where $\delta_{im}=1$ if the points i and m coincide and 0 otherwise.

We have used this theorem to calculate traces only for $l=7$ and when i and m are distinct points. In other cases we have used the theorem as a check on pairs of traces each calculated independently from first principles.

4. Calculation of $\langle P^n Q^2 \rangle$

As with the calculation of $\langle P^n \rangle$, so also with that of $\langle P^n Q^2 \rangle$ we have a correspondence between terms produced on expanding the product and diagrams on the lattice: but now a typical diagram contains not only n lines but also two crosses, on those sites for which we have taken $S_3^{(i)}$ terms from Q^2. When these crosses coincide we shall speak of a double cross. And we first prove:

Theorem II. If D is any diagram and D^* the same diagram together with a double cross, then

$$\mathrm{Tr}\, D^* = \tfrac{1}{3}XY^{\epsilon}\mathrm{Tr}\, D$$

where $\epsilon=1$ if the double cross is not superimposed on D and $\epsilon=0$ if it is.

The proof depends only on the symmetry of the commutation rules with respect to the three components of spin. A consequence of this theorem is that for the purpose simply of calculating a_n, or $\lambda_{n+2}^{(2)}$, diagrams involving double crosses can be ignored ($n \geqslant 1$). For we are finding the coefficient of N in $\mu_{n+2}^{(2)}$: and the theorem implies that the term in N from any diagram together with a double cross *not* lying on it is just the negative of the sum of the terms represented by the same diagram with a double cross superimposed.

Secondly, we prove:

Theorem III. If D is any diagram, and D^+ denotes the same diagram with a *single* cross superimposed (anywhere) on it, then $\mathrm{Tr}\, D^+ = 0$.

This theorem is intimately related to the fact that Z is necessarily an even function of H.

Finally, we prove:

Theorem IV. If D_l^{++} is any (labelled) diagram of l lines and two crosses, at points i and j belonging to the diagram, and D_{l+1} is the diagram obtained by removing the crosses and adding the line ij (whether i and j are neighbouring lattice points or not), then

$$\mathrm{Tr} D_l^{++} = \frac{2}{3}\frac{m}{n}\,\mathrm{Tr}\, D_{l+1}$$

where $m=$ number of terms to which D_l corresponds and $n=$ number of terms to which D_{l+1} corresponds, on permutation of their respective P factors.

The 2 in this equation is the 2 associated with cross-terms in the expansion of Q^2.

As an illustration, we have

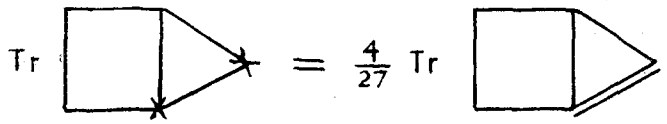

since in this case $m=6!$ and $n=7!/2$.

It is a consequence of theorems III and IV that in calculating $\langle P^n \rangle$ we can, as already asserted, ignore diagrams which fall into two parts on the removal of a single line. For, on replacing this line by crosses at its ends we see that the trace of the diagram necessarily vanishes.

A more important consequence, however, of these theorems is that the traces required for $\langle P^n Q^2 \rangle$ are essentially those needed for $\langle P^{n+1} \rangle$. Nothing further, therefore, need be said concerning their calculation: all the required traces are functions (polynomials) of X only, multiplied by a power of Y which cancels with the factor Y^{-s} in (17) above.

5. General expressions for b and c coefficients

Having found $a_1, a_2, \ldots a_6$, for general spin and any lattice, in terms of X, $=S(S+1)$, and appropriate lattice parameters, we can at once, by inversion of the power-series, find general expressions for the coefficients $b_1, b_2, \ldots b_6$ in the expansion for χ^{-1}, (5) above. Since the expressions for these b coefficients are, due to extensive cancellations, considerably simpler than those for the a coefficients we shall, for brevity, give the general expressions only for the b's. Numerical values of the a's for half-integral values of S from $\frac{1}{2}$ to 3 and for the face-centred and body-centred cubic lattices only, are listed in Appendix II.

It is convenient to write the expressions for the b's in tableau form, the numerical coefficient within the tableau multiplying both the power of X above and the combination of lattice parameters on the left. We find:

$$b_1 = -\frac{2}{3} zX,$$

$$b_2 = \frac{1}{9} zX \left\{ \begin{array}{c|cc} & X & 1 \\ 1 & 4 & 3 \end{array} \right\},$$

$$b_3 = \frac{4}{135} zX \left\{ \begin{array}{c|ccc} & X^2 & X & 1 \\ 1 & -4 & -9 & -6 \\ p_1 & 10 & 5 & \end{array} \right\},$$

$$b_4 = \frac{1}{405} zX \left\{ \begin{array}{c|cccc} & X^3 & X^2 & X & 1 \\ z & & -40 & -45 & \\ 1 & -16 & 64 & 96 & 45 \\ p_1 & -96 & -156 & -54 & \\ p_2 & 80 & 40 & & \end{array} \right\},$$

$$b_5 = \frac{2}{42\,525} zX \left\{ \begin{array}{c|ccccc} & X^4 & X^3 & X^2 & X & 1 \\ \hline z & & 1\,120 & 3\,570 & 3\,780 & \\ 1 & 800 & 80 & -3\,912 & -4\,752 & -1\,728 \\ p_1 & -1\,456 & 12\,936 & 12\,978 & 2\,898 & \\ zp_1 & & -4\,200 & -3\,150 & & \\ p_1^2 & -3\,360 & -3\,360 & -315 & & \\ p_2 & -3\,360 & -6\,160 & -2\,940 & & \\ p_3 & 2\,800 & 1\,400 & & & \end{array} \right\},$$

$$b_6 = \frac{zX}{127\,575} \left\{ \begin{array}{c|cccccc} & X^5 & X^4 & X^3 & X^2 & X & 1 \\ \hline z^2 & & & 5\,880 & 9\,660 & & \\ z & & 8\,064 & -11\,844 & -38\,052 & -29\,862 & \\ 1 & -128 & -12\,960 & -204 & 27\,978 & 29\,196 & 8694 \\ zp_1 & & 24\,640 & 61\,320 & 35\,490 & & \\ p_1 & 24\,960 & -62\,800 & -164\,760 & -108\,900 & -19\,440 & \\ zp_1^2 & & -11\,200 & -6\,440 & & & \\ p_1^2 & 5\,824 & 112\,896 & 81\,648 & 7\,623 & & \\ zp_2 & & -22\,400 & -15\,960 & & & \\ p_2 & -25\,984 & 42\,784 & 66\,612 & 26\,082 & & \\ p_3 & -13\,440 & -27\,440 & -12\,600 & & & \\ p_4 & 11\,200 & 5\,600 & & & & \\ p_1p_2 & -26\,880 & -26\,880 & -5040 & & & \\ q & -4\,480 & -4\,480 & -1\,260 & & & \\ r & & & -840 & -210 & & \end{array} \right\}.$$

Similarly, for the specific heat coefficients, $c_1, c_2, \ldots c_5$, we find:

$$c_1 = \frac{1}{3} \left\{ \begin{array}{c|cc} & X & 1 \\ \hline 1 & & -3 \\ p_1 & 4 & \end{array} \right\},$$

$$c_2 = \frac{4}{15} \left\{ \begin{array}{c|ccc} & X^2 & X & 1 \\ \hline z & & -5 & \\ 1 & -3 & 2 & 3 \\ p_1 & & -5 & \\ p_2 & 5 & & \end{array} \right\},$$

$$c_3 = \frac{2}{27} \left\{ \begin{array}{c|cccc} & X^3 & X^2 & X & 1 \\ \hline z & & & 30 & \\ 1 & & 12 & -12 & -9 \\ p_1 & -48 & 32 & 18 & \\ zp_1 & & -40 & & \\ p_2 & & -20 & & \\ p_3 & 16 & & & \end{array} \right\},$$

$$c_4=\frac{1}{2\,835}\left\{\begin{array}{c|ccccc} & X^4 & X^3 & X^2 & X & 1 \\ \hline z^2 & & & 4\,620 & & \\ z & & 5\,040 & -3\,150 & -8\,190 & \\ 1 & 1\,440 & -2\,880 & -2\,073 & 3\,492 & 1728 \\ zp_1 & & & 13\,860 & & \\ p_1 & 8\,736 & 8\,904 & -12\,348 & -4\,158 & \\ zp_1^2 & & -4\,200 & & & \\ p_1^2 & -15\,120 & 10\,080 & 630 & & \\ zp_2 & & -8\,400 & & & \\ p_2 & -10\,080 & 6\,720 & 5\,985 & & \\ p_3 & & -4\,200 & & & \\ p_4 & 2\,800 & & & & \\ r & & & 105 & & \end{array}\right\},$$

$$c_5=\frac{1}{2\,025}\left\{\begin{array}{c|cccccc} & X^5 & X^4 & X^3 & X^2 & X & 1 \\ \hline z^2 & & & 840 & -7\,980 & & \\ z & & & -7\,728 & 5\,502 & 7\,308 & \\ 1 & & -1\,440 & 4\,224 & 1\,011 & -3\,312 & -1\,242 \\ z^2p_1 & & & 10\,360 & & & \\ zp_1 & & 20\,160 & -14\,840 & -14\,700 & & \\ p_1 & -18\,432 & -16\,672 & 4\,196 & 15\,564 & 3\,636 & \\ zp_1^2 & & & 4\,480 & & & \\ p_1^2 & 34\,944 & 336 & -18\,872 & -2\,142 & & \\ p_1^3 & -6\,720 & 4\,480 & 280 & & & \\ zp_2 & & & 11\,200 & & & \\ p_2 & & 10\,080 & -8\,960 & -5\,775 & & \\ zp_3 & & -5\,600 & & & & \\ p_3 & -6\,720 & 4\,480 & 4\,060 & & & \\ p_4 & & -2\,800 & & & & \\ p_5 & 1\,600 & & & & & \\ zp_1p_2 & & -5\,600 & & & & \\ p_1p_2 & -20\,160 & 13\,440 & 3\,080 & & & \\ r & & & 560 & 105 & & \\ t & & & 140 & & & \end{array}\right\}.$$

These general expressions for the b and c coefficients are given in terms of lattice parameters which have still to be defined. z, of course, is the coordination-number of the lattice. The symbols p_n, q, r, t have the meanings that

$\frac{1}{2(n+2)}zNp_n$ = number of (unlabelled) closed, non-crossing, circuits of $n+2$ points on the lattice,

e.g. $\frac{1}{6}Nzp_1$ = number of triangles the sides of which join neighbouring lattice sites,

$\frac{1}{12}zNq$ = number of (unlabelled) diagrams of the type

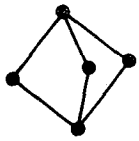

which can be found on the lattice,

$\frac{1}{24}zNr$ = number of (unlabelled) tetrahedra which can be found on the lattice,

$\frac{1}{4}zNt$ = number of (unlabelled) diagrams of the type

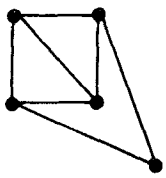

which can be found on the lattice.

Their values for various lattices are tabulated below:

Lattice	z	p_1	p_2	p_3	p_4	p_5	q	r	t
Linear	2	0	0	0	0	0	0	0	0
Honeycomb	3	0	0	0	2	0	0	0	0
Plane square	4	0	2	0	6	0	0	0	0
Plane triangular	6	2	4	10	30	98	0	0	0
Diamond	4	0	0	0	6	0	0	0	0
Simple cubic	6	0	4	0	44	0	0	0	0
Body-centred cubic	8	0	12	0	222	0	18	0	0
Face-centred cubic	12	4	22	140	970	7196	36	4	16

Table 1.

The values were obtained by direct counting on model lattices. They agree in every case with values recently published by Domb and Sykes [10], who used algebraic methods. For consistency with our earlier work, we have kept to our original notation; the conversion to the notation of Domb and Sykes is as follows:

Present work	Domb and Sykes
z	$\sigma+1$
zp_n	$2np_{n+2}$
zq	$12p_{6a}$
zr	$24p_{6d}$
zt	$4p_{7h}$

We have, moreover, used such reduction formulae as

$$p_{5a} = \tfrac{1}{4}zp_1(p_1 - 1),$$
$$p_{6b} = \tfrac{1}{2}zp_1(p_2 - 2p_1 + 2),$$
$$p_{6c} = \tfrac{1}{8}zp_1(zp_1 - 4p_1 + 2),$$

where the symbols on the left are those of Domb and Sykes and those on the right are ours, because such reductions are valid in all the cases in which we are interested and effect a simplification in the general expressions for the a, b and c coefficients.

6. Checking procedures

It is, of course, most important in work of this kind, entailing a large number of individual calculations each of some complexity, that there should be adequate checks which can be applied to the final results. We are fortunate, however, in having performed all the trace calculations for $S = \frac{1}{2}$ by an entirely different method (Rushbrooke and Wood [6] and unpublished work on a_6) and for $S = \frac{1}{2}$ we agree entirely with the independent work of Domb and Sykes [7]. We may therefore assume that the results for $S = \frac{1}{2}$ are known, and the first check on the general formulae is obtained by putting $X = \frac{3}{4}$.

This check, however, is not sufficient. For, rather surprisingly, the results given by Brown [5] for a_5 for open lattices, general spin, satisfy this check but disagree with our general expression. This is because the discrepancy amounts to $(8/1215)\, zp_2X^3\,(4X-3)$, which vanishes when $X = \frac{3}{4}$.

We therefore consider certain finite lattices, to which the general theory still applies, and for which we can calculate the eigenvalues of $\mathscr{H}$, and their degeneracies, explicitly, and thence find, Z, χ and C as functions of $1/T$. These finite lattices may all be described as n-point lattices, an n-point lattice comprising n points and all $\frac{1}{2}n(n-1)$ links between them (so that every point is a neighbour of all the others); that they are not geometrically possible in three-dimensional space after $n = 4$ (tetrahedron) is immaterial. We have dealt with the cases $n = 2, 3, \ldots 7$, when $S = 1$. It would be possible, but laborious, to consider higher values of S. In every case we get agreement with our general formulae, which can therefore only be in error by terms involving the factor $(4X-3)(X-2)$: which is highly unlikely. An indication of the method of finding the eigenvalues of $\mathscr{H}$, and their degeneracies, for an n-point lattice is given in Appendix III.

7. Curie temperatures

The method originally used by Opechowski, and Zehler, for estimating the Curie temperature from a knowledge of the first few a or b coefficients was to find the smallest positive real root of the equation

$$1 + b_1x + b_2x^2 + \ldots = 0 \qquad (18)$$

(where the left-hand side is curtailed after the known coefficients). Denoting this by x^*, $\chi^{-1} = 0$ when $\theta = 1/x^*$, so that $1/x^*$ is the estimate of the Curie temperature.

In our 1955 paper we observed that what we are really seeking is the radius of convergence of the power-series for χ. The Opechowski–Zehler method should

give a sequence of estimates for θ_c, as more and more b's are included, which converge to the true value: but it may be more satisfactory, as well as simpler, to attempt directly to estimate the radius of convergence of the series

$$1 + a_1 x + a_2 x^2 + \ldots \tag{19}$$

from the coefficients a_n.

For $S = \frac{1}{2}$ and $S = 1$ we have, in fact, used both methods: but since estimates based on the a-coefficients do in general form a smoother sequence we have confined attention to the a-coefficients for $S = \frac{3}{2}$, 2, $\frac{5}{2}$ and 3. Successive estimates based on equation (18) are, however, perhaps worth tabulating. Table 2 lists, for $S = \frac{1}{2}$ and $S = 1$, for $m = 1, 2, \ldots 6$ and for various lattices, the reciprocal of the smallest positive real root of equation (18) curtailed after the coefficient b_m. If the appropriate root happens to be imaginary we have determined its modulus and the reciprocal of this is tabulated in brackets (e.g. all two-dimensional lattices when $m = 2$).

Lattice		$m=1$	$m=2$	$m=3$	$m=4$	$m=5$	$m=6$
Linear	$S=\frac{1}{2}$	1·0	(1·0)	0·7959	0·6043	(0·8266)	0·7411
	$S=1$	2·6667	(2·2111)	1·5089	1·7015	(1·6695)	(1·6159)
Honey-comb	$S=\frac{1}{2}$	1·5	(1·2247)	1·0	1·0723	(1·0861)	(0·9757)
	$S=1$	4·0	(2·7080)	2·1236	2·5604	(2·1504)	(2·5746)
Plane square	$S=\frac{1}{2}$	2·0	(1·4142)	1·2531	1·0951	(1·1030)	(1·1036)
	$S=1$	5·3333	(3·1269)	3·2059	(2·1028)	2·9669	2·7319
Triangular	$S=\frac{1}{2}$	3·0	(1·7321)	(3·4551)	1·7524	1·8730	(1·5754)
	$S=1$	8·0	5·1547	(4·7919)	(4·4849)	4·3832	4·5181
Diamond	$S=\frac{1}{2}$	2·0	(1·4142)	1·2531	1·4471	(1·3017)	(1·3352)
	$S=1$	5·3333	(3·1269)	3·2059	3·6203	3·1849	(3·3284)
Simple cubic	$S=\frac{1}{2}$	3·0	(1·7321)	2·0	1·9305	1·8339	(1·7837)
	$S=1$	8·0	5·1547	5·9316	5·3631	5·6814	5·1856
Body-centred	$S=\frac{1}{2}$	4·0	2·0	2·9507	2·3918	2·7873	2·4825
	$S=1$	10·6667	8·3148	8·6617	7·8161	8·1753	7·7695
Face-centred	$S=\frac{1}{2}$	6·0	4·7321	4·2618	4·2426	4·2639	4·2322
	$S=1$	16·0	13·8878	13·0970	12·7394	12·5482	12·4345

Table 2.

For the face-centred lattice the behaviour, though oscillatory when $S = \frac{1}{2}$, is very regular and satisfactorily convergent. For other lattices the sequence of these roots is, on the whole, more irregular than that of the coefficients a_n, and we have preferred to base our estimates of the Curie temperatures primarily on the values of the a-coefficients.

Except for the linear lattice, and the honeycomb lattice when $S=\frac{1}{2}$, all the coefficients a_n, whatever the lattice and whatever the spin, are positive. Consequently the radius of convergence of the series (19) is determined by a singularity on the positive real axis, and the Curie temperature, θ_c, should be given by the limit, as $n\to\infty$, of any of the quantities $a_n^{1/n}$, a_n/a_{n-1}, $(a_n/a_{n-2})^{1/2}\ldots$. Which of these is the most suitable only trial can show: we shall naturally use whatever set shows the most regular behaviour for $n=1, 2, \ldots 6$. In fact, owing to an oscillatory behaviour in the coefficients it is generally the set $(a_n/a_{n-2})^{1/2}$, $n=2, 3, \ldots 6$,

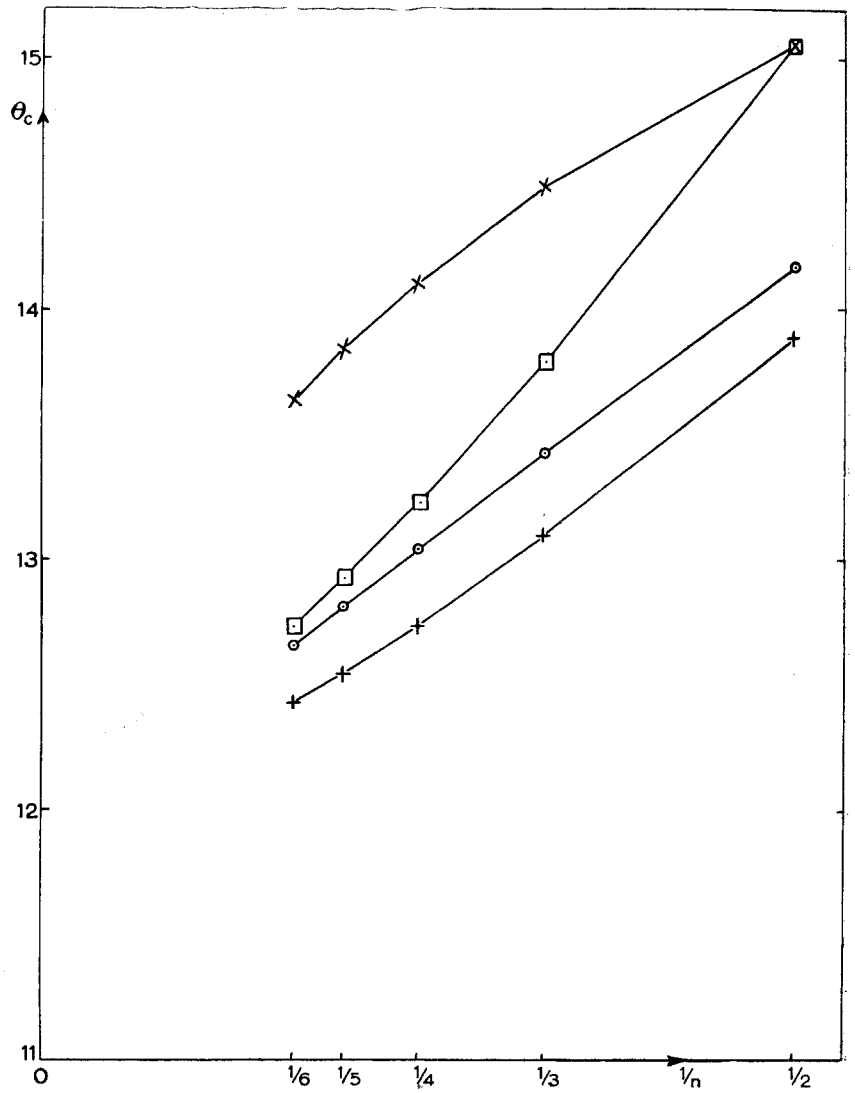

Figure 1. Face-centred cubic lattice, $S=1$.

× $a_n^{1/n}$.

□ $(a_n/a_{n-2})^{1/2}$.

⊙ a_n/a_{n-1}.

\+ Roots of $1/\chi=0$.

with $a_0 = 1$, which behaves most smoothly and is most suitable for extrapolation: but we have always considered all three of these sequences. Figure 1, although not entirely typical, illustrates quite well the procedure we have adopted: it refers to the face-centred cubic lattice and $S = 1$, and the four sequences, as we descend the diagram, are, respectively, $a_n^{1/n}$, $(a_n/a_{n-2})^{1/2}$, a_n/a_{n-1}, and the successive estimates of θ_c as obtained from equation (18) and given numerically in the last line of table 1. As ordinate we have used $1/n$ (points for $n = 1$ are not shown), and we have to extrapolate the sequences to $1/n = 0$. For this purpose we have always drawn up a Neville table and proceeded numerically, though necessarily judgement must be exercised and is more important than routine procedure. In this case we estimate $\theta_c = 12{\cdot}0$, to within one per cent.

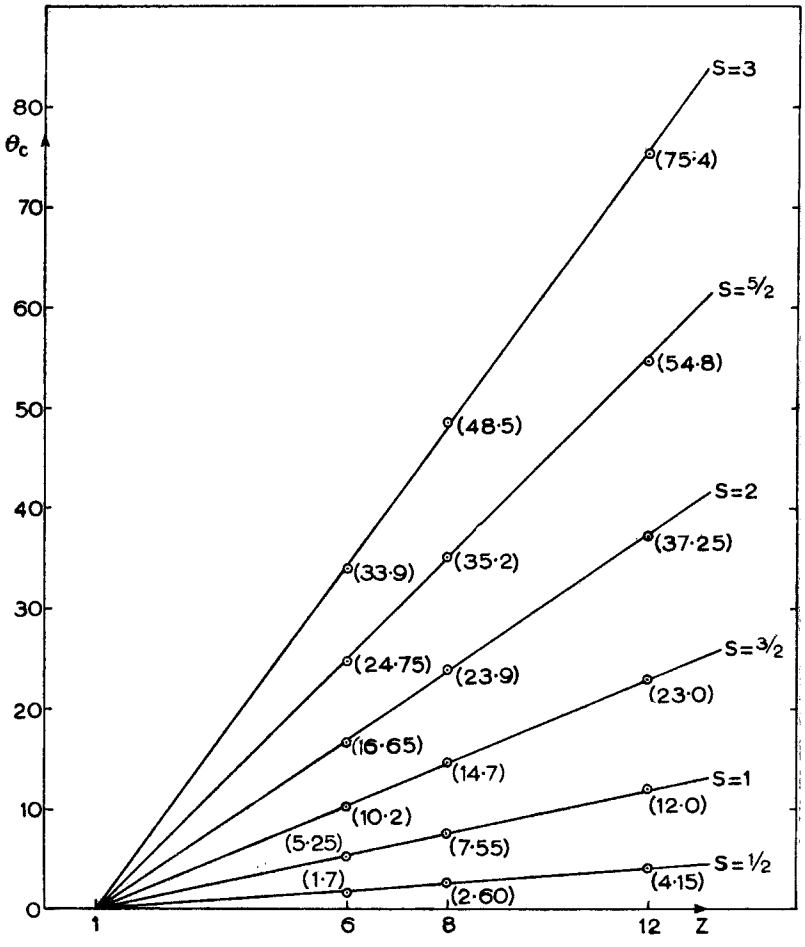

Figure 2.

In this way, we have estimated the Curie temperatures, θ_c, for the simple ($z = 6$), body-centred ($z = 8$) and face-centred ($z = 12$) cubic lattices, for $S = \frac{1}{2}$, 1, $\frac{3}{2}$, 2, $\frac{5}{2}$ and 3: figure 2 shows these estimates (which may be regarded as known to approximately one per cent, although generally we are rather more confident than

this and would incline to say $\pm 0{\cdot}1$) plotted against the lattice coordination-number, z. The numerical values (centre of any range of uncertainty) are given on the diagram.

We observe the remarkable, and unexpected, feature that, for any spin, the Curie points of the three cubic lattices lie on straight lines all cutting the z-axis at $z=1$. Moreover, if we determine the gradients, m, of these lines, writing $\theta_c = m(z-1)$, and plot m against X $(=S(S+1))$ we again obtain extraordinary linearity, as shown in figure 3.

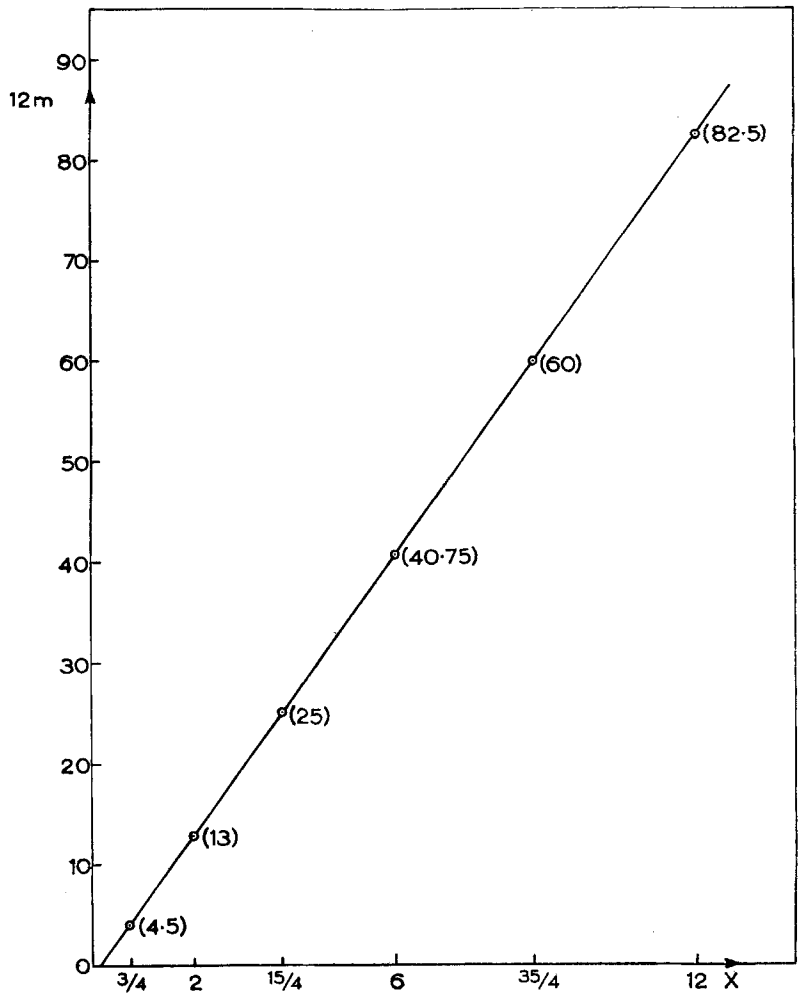

Figure 3.

These two properties of the estimated Curie temperatures can be summarized in the simple equation

$$\theta_c = \frac{5}{96}(z-1)(11X-1), \tag{20}$$

which reproduces all our values, for these cubic lattices, to within about one per

cent, i.e. to within a fairly conservative estimate of their reliability†. We regard equation (20) more in the nature of a mnemonic than as having any deep significance, and certainly it is not valid for two-dimensional lattices. Whether it is again approximately correct for the three-dimensional diamond lattice is uncertain, since we cannot make very reliable estimates of the Curie temperatures from the a-coefficients in this case. But the values given by equation (20) with $z=4$ are certainly by no means unreasonable.

Before leaving this discussion of the Curie temperatures, there are three points which may conveniently be made here. The first concerns the hexagonal close-packed lattice. As Domb and Sykes have observed already [11], the lattice parameter which we have called q, in table 1 above, has the value 37 for the hexagonal close-packed lattice in contrast to 36 for the face-centred cubic lattice. Essentially, this is because the diagram

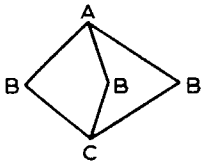

can, for the hexagonal lattice, occur with the three points B at the vertices of a triangle in a close-packed plane and with A and C at lattice sites in parallel planes above and below this: which is not possible for the face-centred cubic lattice. Consequently the values of a_6 and b_6 are slightly different for the hexagonal close-packed and face-centred cubic lattices. The difference, however, is extremely small: the a_6 values are greater for the hexagonal close-packed lattice than for the face-centred cubic lattice, but by less than 2 in 10^5 when $S=\frac{1}{2}$ and less than 1 in 10^5 when $S=1$. Likewise with the entries in the bottom right-hand corner of table 2: for the hexagonal close-packed lattice these read 4·2326 and 12·4347, for $S=\frac{1}{2}$ and 1 respectively. These differences are far too small to enable any conclusions to be drawn concerning possible differences in the Curie temperatures for these two lattices.

Secondly, it is of some interest to compare our estimated Curie temperatures with those given by the constant-coupling approximation of Kasteleijn and van Kranendonk [12]. Their estimates of θ_c, given in table 2 of their paper, are in all cases approximately 13 per cent greater than those which we have found.

† The equation of the line in figure 3, determined by least-squares, is

$$\theta_c=(z-1)(0\cdot579X-0\cdot072).$$

There are a number of possible formulae of the type of (20) which cover this adequately well. For the body-centred and face-centred lattices we have determined the behaviour of θ_c for large X, by retaining only the greatest power of X in the expressions for the a-coefficients. In this way we find

body-centred cubic lattice $\quad\theta_c\simeq(z-1)(0\cdot586X+\text{constant})$,

face-centred cubic lattice $\quad\theta_c\simeq(z-1)(0\cdot578X+\text{constant})$.

These equations enable us to draw the limiting asymptotes for large S in figures 4 and 5 below. They also confirm the minor features of figure 2, wherein the points for the body-centred lattice tend to lie slightly above the lines of the diagram, just as those for the simple cubic lattice tend to lie slightly below these lines.

Finally, we would observe that there is no evidence that the two-dimensional lattices (or even, though more doubtfully, the linear lattice) do not have Curie temperatures. Admittedly, firm conclusions are more difficult to draw from the coefficients in these cases: but with the plane triangular lattice, for example, convergence is reasonably good and suggests, for all spin values, a Curie temperature approximately two-thirds of that for the three-dimensional simple cubic lattice. We shall not go into further details here: suffice it to add that, of course, such a high-temperature transition point does not imply anything at all about the magnetic state of the lattice at very low temperatures. Orthodox spin-wave theory precluded two-dimensional ferromagnetics at low temperatures (but see Frank [13], on which work we refrain from further comment here).

8. Susceptibility above the Curie temperature

Equation (5), above, may be rewritten as

$$\frac{1}{\bar{\bar{\chi}}} = \tau + \frac{b_1}{\theta_c} + \sum_{n \geqslant 2} \frac{b_n}{\theta_c{}^n} \frac{1}{\tau^n} \tag{21}$$

where $\tau = T/T_c$

and $$\bar{\bar{\chi}} = \frac{3}{S(S+1)} \bar{\chi} \theta_c = \frac{3\boldsymbol{k}T_c}{S(S+1)Ng^2\beta^2} \chi.$$

With this choice of scale, a plot of $1/\bar{\bar{\chi}}$ against τ tends to a linear asymptote having unit gradient, and passing through the Curie–Weiss point $\theta = -b_1 = \frac{2}{3} z S(S+1)$. In order to plot inverse susceptibility against temperature more completely above the Curie point, we have considered the successive approximations obtained by curtailing equation (21) after $n = 2, 3, \ldots 6$, and have attempted to extrapolate from these successive approximations. Numerically, we have considered successive estimates of $1/\bar{\bar{\chi}}$ for a given value of τ and plotted these against $1/n$: judgement must then be exercised in estimating their ultimate limit. Likewise we have attempted to extrapolate on the gradients of the curves at $\tau = 1$, where $1/\bar{\bar{\chi}} = 0$. While we would not claim more than a few per cent accuracy in the final curves given (full lines) in figures 4 and 5, each of these curves does in fact accord well with direct visual extrapolation, graphically, on the set of curves representing successive approximations to $1/\bar{\bar{\chi}}$. The lower, broken, lines in figures 4 and 5 show the Curie–Weiss asymptotes obtained by retaining only the first two terms on the right-hand side of (21).

The most noteworthy features of these curves are their insensitivity to either S or the particular lattice (face-centred or body-centred) concerned. Incidentally, $S = 3$ is very nearly equivalent to letting $S \to \infty$, and curves for $S = \frac{3}{2}$, 2, $\frac{5}{2}$ would lie between those for $S = 1$ and $S = 3$. In all cases the initial gradient, at the Curie point, appears to be close to 0·3 (with the final gradient scaled to have the value unity). Very similar behaviour has been reported recently for the Ising model by Domb and Sykes [14]: and in figures 4 and 5 we have added the susceptibility curves for the ordinary two-valued (' up or down ') Ising model—curves marked I. For the body-centred lattice this is based on unpublished calculations of Rushbrooke and Scoins, and it agrees with the curve given in [14]. For the face-centred lattice the Ising curve has been taken from figure 3 of Domb and Sykes, with the change of scale required to give the asymptote unit gradient.

To the theoretical curves of figures 4 and 5 we have added experimental data for iron and nickel, respectively. To convert from a measured value of $1/\chi$ to the plotted value of $1/\bar{\bar{\chi}}$ we have to multiply the measured value by

$$S(S+1)N_0g^2\beta^2/3M\boldsymbol{k}T_c,$$

where N_0 is Avagadro's number and M the atomic weight. Thus the plot of the experimental points depends on the choice adopted for S and g. (We notice that the exchange interaction, J, does not enter into this scale factor.) For both iron

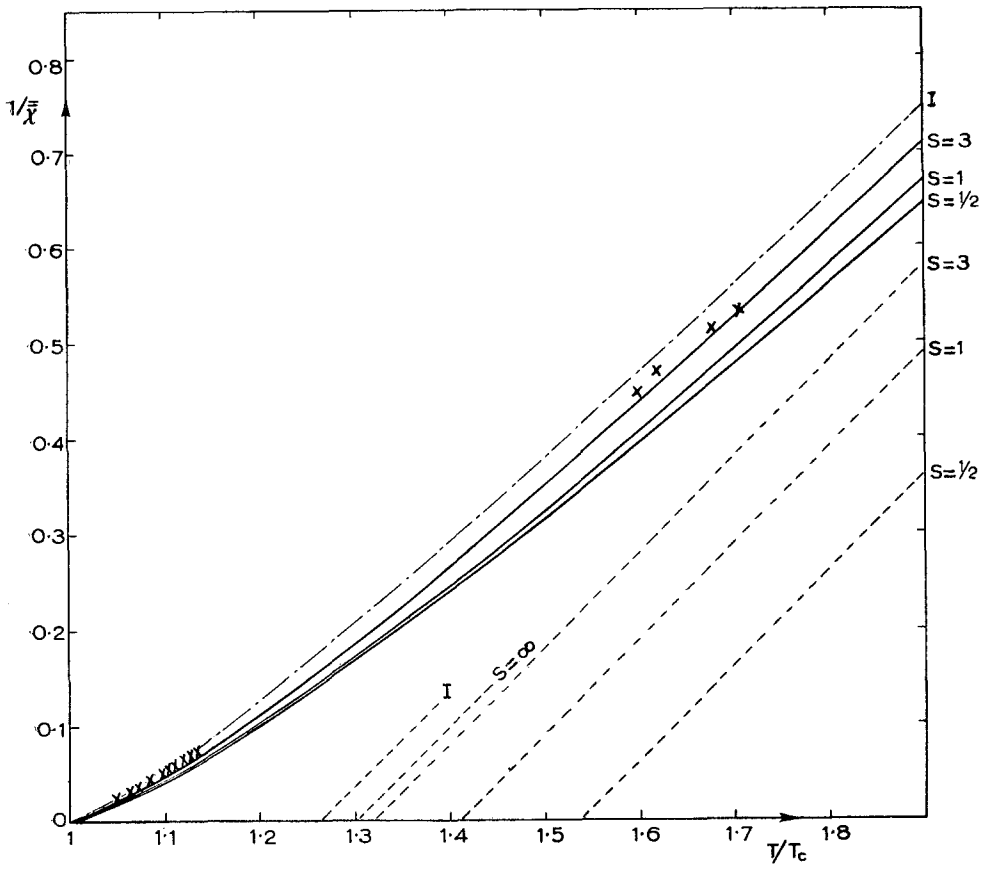

Figure 4. Body-centred cubic lattice.
× Fe values, Sucksmith and Pearce.

and nickel we have taken $g=2$: for nickel we have taken $S=\frac{1}{2}$ and for iron we have taken $S=1$. The experimental data are those of Sucksmith and Pearce [15] for iron in its two body-centred phases (β and δ), and for nickel we have used the data of Sucksmith and Pearce [15] and Weiss and Forrer—taken from Néel [16]. For the Curie temperatures, T_c, we have taken the generally accepted values of 1043°K and 631°K for iron and nickel respectively (Stoner [17]). We shall discuss the two comparisons separately·

First iron. The agreement is very gratifying. That the experimental points lie in fact closer to the curve I than to the Heisenberg curve for $S = 1$ is immaterial: we have used no adjustable parameters to obtain a fit and in any case must recognize that however accurately the statistical side of the calculations is performed the Heisenberg model does only crude justice to the quantum mechanics of an assembly of localized electron pairs. Since for iron, as distinct from nickel, this localized picture seems to be basically satisfactory (Griffith [18], Mott and Stevens [19]), however, we may feel that in this case reasonable agreement is not altogether surprising.

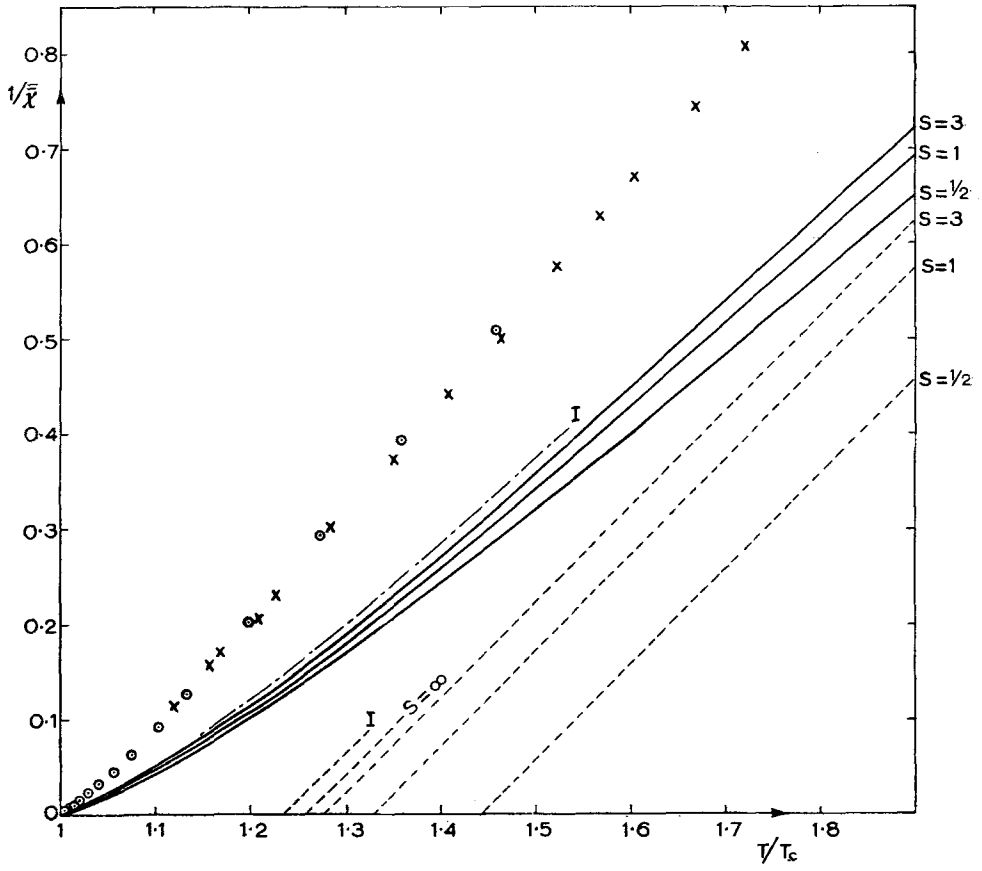

Figure 5. Face-centred cubic lattice.
× Ni values, Sucksmith and Pearce.
⊙ Ni values, Weiss and Forrer.

With nickel, the situation is rather different. As plotted in figure 5 the experimental points certainly do not accord with the theoretical curves. However, if we recall that for nickel the number of effective magnetic electrons, as determined from the saturation magnetization, is only 0·6 per atom, and therefore multiply the theoretical estimate of χ by 0·6 or, which comes to the same thing for figure 5, multiply the experimental values of $1/\bar{\chi}$ by 0·6, we again obtain a situation very

much like that of figure 4. When scaled down in this way, the experimental points coincide very closely with the $S=3$ Heisenberg curve up to $T/T_c=1{\cdot}2$ and then drift slowly across to reach the $S=\frac{1}{2}$ curve at about $T/T_c=1{\cdot}6$. Again we would not wish to draw a significant difference between these curves. Domb and Sykes [14] have already shown how close the agreement can be made by a suitable choice of scale. What is surprising is that the localized model, whether Heisenberg or Ising, does sufficient justice, when scaled in this way, to the quantum mechanics of the magnetic electrons in nickel to give reasonable agreement with the susceptibility above the Curie temperature. For it is generally agreed that these electrons should be regarded as non-localized (see Stoner [17]).

Finally, returning to iron, we would note that taking $\theta_c=7{\cdot}55$ as appropriate to the Heisenberg model with $S=1$ for the body-centred lattice, the Curie temperature of 1043°K corresponds to a J value equal to $1{\cdot}19\times10^{-2}$ ev or 274 cal mole^{-1}.

9. Magnetic specific heat

Numerical values of the coefficients c_n of equation (14), for the body-centred and face-centred cubic lattices only, are tabulated in Appendix IV. It is in fact only for the face-centred lattice that the coefficients (with one exception when $S=\frac{1}{2}$) are all positive. For this particular lattice the radius of convergence of equation (14) appears to be significantly close to that of equation (4), for the susceptibility; and a magnetic specific heat anomaly at the Curie point is fairly clearly indicated. For other lattices we have insufficient specific heat coefficients to enable firm conclusions easily to be drawn. Undoubtedly these coefficients would repay further consideration, particularly for the anti-ferromagnetic problem: but we shall not discuss them further here.

10. The antiferromagnetic problem

We have already made passing reference, both in the Introduction and immediately above, to the use that can be made of these coefficients in antiferromagnetic problems, when J is negative. The paper of Danielian and Stevens illustrates a fruitful approach, though it would appear that the results can be obtained rather more simply.

In essence, Danielian and Stevens start with equation (4) with $1/\theta$ replaced by z, i.e.

$$\bar{\chi}=\tfrac{1}{3}S(S+1)z(1+a_1z+a_2z^2+\ldots) \tag{22}$$

and observe that whereas in the ferromagnetic problem we require the singularity, F, of the right-hand side lying nearest to the origin on the positive real axis, in the antiferromagnetic problem we shall be concerned with the singularity (if any) A, of the right-hand side of (22) lying nearest to the origin on the negative real axis. Since the a's are positive, F will lie closer to the origin, and (22) will require analytic continuation outside its circle of convergence in order that we may reach the point A. For this purpose they suggest the transformation

$$\frac{1}{w}=d+\frac{1}{z}$$

where d is a constant (θ in their paper, but we use d here to avoid confusion with our use of θ for reduced temperature).

Having thus obtained a series for $\bar{\chi}$ in powers of w which is valid (converges) for values of w corresponding to values of z beyond the circle of convergence of (22) they are in a position to evaluate $\bar{\chi}$ for the range of temperature $(1/|z|)$ of interest in the antiferromagnetic problem, and they conclude by plotting $1/\bar{\chi}$ against temperature in this case.

However, if interest centres in $1/\bar{\chi}$ (as it can always be made to do) it would seem simpler to start with equation (5). This series certainly does not break down at the point F, for here $1/\bar{\chi}$ is zero, not infinite. Writing (5) as

$$\frac{z}{\bar{\chi}} = \frac{3}{S(S+1)}(1 + b_1 z + b_2 z^2 + \ldots) \tag{23}$$

the corresponding antiferromagnetic series is

$$\frac{z}{\bar{\chi}} = \frac{3}{S(S+1)}(1 - b_1 z + b_2 z^2 - b_3 z^3 + \ldots)$$

or

$$\frac{1}{\bar{\chi}} = \frac{3}{S(S+1)} t\left(1 - \frac{b_1}{t} + \frac{b_2}{t^2} - \frac{b_3}{t^3} + \ldots\right) \tag{24}$$

where, to avoid ambiguity, we have denoted $kT/|J|$ by t (real, positive, reduced temperature for the antiferromagnetic problem).

The only reason why (24) cannot be used as it stands to plot $1/\bar{\chi}$ against t is that such a power-series ceases to be appropriate when t is small—for the final term at which we have to curtail the series then dominates the calculation. But we can avoid this difficulty quite simply by a change of origin. It we write $t = t' - d$ and convert to a power-series in $1/t'$ then $t \to 0$ simply corresponds to $t' \to d$ and the power-series in $1/t'$ will remain valid.

This is, of course, precisely equivalent to the transformation of Danielian and Stevens (with $1/t' = w$), but a more direct approach. The fact that rather different curves (see figure in Danielian and Stevens) result from different choices of d is, of course, due to the inevitable curtailment of the series (24).

For numerical evaluation of the general expressions for the a, b and c coefficients, particularly for the higher spin values, and for numerical evaluation of the approximations to $1/\bar{\chi}$, we used the digital computer FERDINAND of the Durham University Computing Laboratory. We are grateful to the Director, Dr. Page, for the facilities of the Laboratory and are particularly indebted to Dr. J. Eve for advice and assistance with the programming.

One of us (P. J. W.) wishes to thank the Council of King's College for a research award and Messrs. George Angus and Co. Ltd. for the, subsequent, award of a Studentship.

Appendix I

The following basic traces, determined from explicit representations of the spin matrices, suffice for the calculations reported in this paper. We use the short-hand notation in which Tr (*123*), for example, stands for Tr $(S_1 S_2 S_3)$. We observe that an even (cyclic) permutation of the suffices *1*, *2*, *3* leaves the spin commutation rules unchanged, and so does an odd (anticyclic) permutation together with the transformation $\mathbf{S} \to -\mathbf{S}$. Thus, for example Tr (*132*) = − Tr (*123*)

and $\mathrm{Tr}(\mathit{1331}) = \mathrm{Tr}(\mathit{1122})$. We list only basic traces, from which others follow on using these rules, and omit those which vanish. $X = S(S+1)$. $Y = 2S+1$.

$$\mathrm{Tr}(\mathit{11}) = \frac{1}{3}XY$$

$$\mathrm{Tr}(\mathit{123}) = \frac{1}{6}iXY$$

$$\mathrm{Tr}(\mathit{1111}) = \frac{1}{15}XY(3X-1)$$

$$\mathrm{Tr}(\mathit{1122}) = \frac{1}{30}XY(2X+1)$$

$$\mathrm{Tr}(\mathit{1212}) = \frac{1}{15}XY(X-2)$$

$$\mathrm{Tr}(\mathit{11123}) = \frac{1}{30}iXY(3X-1)$$

$$\mathrm{Tr}(\mathit{11213}) = \frac{1}{30}iXY(X-2)$$

$$\mathrm{Tr}(\mathit{111111}) = \frac{1}{21}XY(3X^2-3X+1)$$

$$\mathrm{Tr}(\mathit{111122}) = \frac{1}{210}XY(6X^2+8X-5)$$

$$\mathrm{Tr}(\mathit{111212}) = \frac{1}{210}XY(6X^2-13X+2)$$

$$\mathrm{Tr}(\mathit{112112}) = \frac{1}{210}XY(6X^2-20X+16)$$

$$\mathrm{Tr}(\mathit{112233}) = \frac{1}{210}XY(2X^2-9X+10)$$

$$\mathrm{Tr}(\mathit{123132}) = \frac{1}{210}XY(2X^2-9X+10)$$

$$\mathrm{Tr}(\mathit{112323}) = \frac{1}{210}XY(2X^2-2X-4)$$

$$\mathrm{Tr}(\mathit{112332}) = \frac{1}{210}XY(2X^2+19X-11)$$

$$\mathrm{Tr}(\mathit{123123}) = \frac{1}{210}XY(2X^2-30X+17)$$

$$\mathrm{Tr}(\mathit{1111123}) = \frac{1}{42}iXY(3X^2-3X+1)$$

$$\mathrm{Tr}(\mathit{1111213}) = \frac{1}{210}iXY(9X^2-23X+10)$$

$$\mathrm{Tr}(\mathit{1112113}) = \frac{1}{210}iXY(3X^2-10X+8)$$

$$\mathrm{Tr}(\mathit{1112223}) = \frac{1}{420}iXY(18X^2+3X-8)$$

$$\mathrm{Tr}(\mathit{1121223}) = \frac{1}{420}iXY(14X^2-35X+14)$$

$$\mathrm{Tr}(\mathit{1211223}) = \frac{1}{420}iXY(10X^2-31X+22)$$

$$\mathrm{Tr}\,(2111223) = \frac{1}{420} iXY\,(6X^2 - 13X + 2)$$

$$\mathrm{Tr}\,(1221123) = \frac{1}{420} iXY\,(2X^2 + 47X - 32)$$

$$\mathrm{Tr}\,(1212123) = \frac{1}{420} iXY\,(6X^2 - 13X + 2)$$

$$\mathrm{Tr}\,(2112123) = \frac{1}{420} iXY\,(2X^2 - 9X + 10).$$

Appendix II

Values of $a_1, a_2, \ldots a_6$ (descending the columns) for the body-centred and face-centred cubic lattices. $a_0 = 1$.

	Body-centred	Face-centred
$S = \frac{1}{2}$	4·0	6·0
	12·0	30·0
	34·6667	138·0
	95·8333	611·25
	262·7	2658·55
	708·0417	11432·5125
$S = 1$	10·6667	16·0
	94·2222	226·6667
	815·4074	3043·5556
	6742·7160	39696·2963
	55268·1877	508532·3062
	445315·4678	6436787·9243
$S = \frac{3}{2}$	20·0	30·0
	340·0	810·0
	5683·3333	20878·0
	91162·5	524331·25
	1450059·3667	12952039·55
	22684384·8861	316344057·2458
$S = 2$	32·0	48·0
	880·0	2088·0
	23842·1333	86963·2
	620572·8	3533867·2
	16030091·9467	141348884·48
	407410376·3911	5592392606·9333
$S = \frac{5}{2}$	46·6667	70·0
	1882·2222	4456·6667
	74855·4074	272077·5556
	2862918·5494	16218187·5463
	108692104·3988	951946301·7895
	4061214171·7761	55282299243·5479
$S = 3$	64·0	96·0
	3552·0	8400·0
	194474·6667	705408·0
	10246133·3333	57865200·0
	535953056·9143	4675200497·3714
	27595469888·0	373773684115·2

Appendix III

In this Appendix we show how to obtain the eigenvalues and degeneracies of

$$R=\sum_{i<j=1}^{N}\mathbf{S}^{(i)}.\mathbf{S}^{(j)}+\alpha\sum_i S_3^{(i)} \quad (\alpha=a \text{ constant}).$$

The operator R may be rewritten as

$$\begin{aligned}R&=\tfrac{1}{2}\Big(\sum_i \mathbf{S}^{(i)}\Big)^2-\tfrac{1}{2}\sum_i \mathbf{S}^{(i)2}+\alpha\sum_i S_3^{(i)}\\&=\tfrac{1}{2}\mathbf{J}^2-\tfrac{1}{2}\sum_i S^{(i)2}+\alpha J_3\end{aligned}$$

where $$\mathbf{J}=\mathbf{S}^{(1)}+\mathbf{S}^{(2)}+\ldots+\mathbf{S}^{(N)}.$$

Now the operators $\mathbf{S}^{(1)2}$, $\mathbf{S}^{(2)2}$, $\ldots$ $\mathbf{S}^{(N)2}$, $\mathbf{J}$, J_3 form a commuting set (not, however, complete). Let the simultaneous eigenfunctions of this set be denoted by $\psi(j,m)$ where

$$\begin{aligned}\mathbf{S}^{(i)2}\psi(j,m)&=S(S+1)\psi(j,m) \qquad (\text{all } i)\\ \mathbf{J}^2\psi(j,m)&=j(j+1)\psi(j,m)\\ J_3\psi(j,m)&=m\psi(j,m).\end{aligned}$$

Let the functions $\psi(j,m)$ be ordered as follows: the ψ's with equal m are grouped together, the group with largest m coming first etc. Within one of these groups ψ's with equal j are grouped together, the group having largest j coming first etc. The ordering of ψ's with fixed j and m is immaterial.

The sizes of the blocks of constant m are given by the coefficients of x^m in $(x^S+x^{S-1}+\ldots+x^{-S})^N$, since they are the numbers of solutions of

$$m_1+m_2+\ldots+m_N=m$$

where $m_1, m_2, \ldots m_N$ may take the values $S, S-1, \ldots -S+1, -S$. And the number of states with given j and m is the same for all m. For suppose the states with given j and m are $\psi_1(j,m), \psi_2(j,m)\ldots\psi_n(j,m)$, then applying the operators $J^{\pm}=J_1\pm J_2$ to these we obtain $\psi_1(j,m\pm1),\ldots\psi_n(j,m\pm1)$, no two of which can be the same.

Now the operator R is diagonal in the ψ scheme since

$$R\psi(j,m)=[\tfrac{1}{2}j(j+1)-\tfrac{1}{2}NS(S+1)+\alpha m]\psi(j,m)=E(j,m)\psi(j,m).$$

For a given m, j may take the values $NS, NS-1, \ldots |m|$, and for states of given j and m the eigenvalues of R are equal.

Let

$$(x^S+x^{S-1}+\ldots+x^{-S})^N=\sum_{m=-NS}^{NS}a_m x^m.$$

Then a_m is the number of states having a given m. This number is made up of states having different j's ($j=NS, NS-1, \ldots |m|$).

a_{NS} = number of states with $m=NS$ and $j=NS$,

a_{NS-1} = number of states with $m=NS-1$ and $j=NS$ or $j=NS-1$, etc.

But we have seen that the number of states with $m=NS, j=NS$ is equal to the number of states with $m=NS-1, j=NS$. By continually using this fact we obtain:

Number of states with $m=NS$, $j=NS$ is a_{NS},
Number of states with $m=NS-1$, $j=NS$ is a_{NS},
Number of states with $m=NS-1$, $j=NS-1$ is $a_{NS-1}-a_{NS}$,
Number of states with $m=NS-2$, $j=NS$ is a_{NS},
Number of states with $m=NS-2$, $j=NS-1$ is $a_{NS-1}-a_{NS}$,
Number of states with $m=NS-2$, $j=NS-2$ is $a_{NS-2}-a_{NS-1}$ etc.

This number of states gives the degeneracy of $E(j,m)$.

Appendix IV

Values of the coefficients $c_1, c_2, \ldots c_5$ (descending the columns) of equation (14) for the body-centred and face-centred cubic lattices. $c_0 = 1$.

	Body-centred	Face-centred
$S = \frac{1}{2}$	−1·0	3·0
	1·75	1·25
	2·5	−5·8333
	5·3125	23·4375
	−6·4458	210·7292
$S = 1$	−1·0	9·6667
	41·3333	73·3333
	−34·4444	617·4074
	1328·1481	5733·5802
	−1162·2074	56702·9383
$S = \frac{3}{2}$	−1·0	19·0
	176·55	324·05
	−174·8333	5803·5
	23824·9458	106659·4042
	−27544·9592	2029793·4825
$S = 2$	−1·0	31·0
	487·2	903·2
	−507·3333	27034·0
	181268·5333	819051·4667
	−227869·7867	25496671·76
$S = \frac{5}{2}$	−1·0	45·6667
	1075·8833	2003·3833
	−1145·9444	89310·9074
	884475·4035	4010824·2939
	−1154509·7999	184445348·5208
$S = 3$	−1·0	63·0
	2068·0	3860·0
	−2230·0	238836·6667
	3269828·5714	14853668·5714
	−4356540·1333	944242800·6667

On a déterminé, en utilisant le modèle d'un corps ferromagnétique dû à Heisenberg, les six premiers coefficients du développement de la susceptibilité χ et de son inverse χ^{-1} en puissances croissantes de la température réciproque, pour une valeur quelconque S du spin et pour un réseau quelconque. Les cinq premiers coefficients relatifs à la chaleur spécifique magnétique, C, ont été trouvés aussi. On donne, pour les réseaux cubiques centrés, et à faces centrées, un tableau des coefficients de χ et C calculés pour des valeurs semi-entières de S allant de $\frac{1}{2}$ à 3.

On a estimé, à partir de ces coefficients, les températures du Curie réduites $\theta_c = kT_c/J$. On trouve, pour les réseaux cubiques simple, centré, et à faces centrées, que la formule:

$$\theta_c = \tfrac{5}{96}(z-1)(11X-1)$$

rend compte des températures de Curie estimées avec assez de précision. Ici, $X = S(S+1)$, et z est le numéro de coordination du réseau.

On trouve que les courbes théoriques de l'inverse de la susceptibilité en fonction de la température, au-dessus du point de Curie, si elles sont réduites à une échelle convenable, sont pratiquement indépendantes de la valeur du spin et de la structure précise du réseau.

Le rapport des pentes initiales et finales est environ 0,3. On compare avec les valeurs expérimentales de χ^{-1} pour le fer et le nickel. Le fer étant représenté par un modèle de Heisenberg avec $S=1$, la température de Curie observée correspond alors à une valeur de J égale à $1{,}19\times10^{-2}$ ev.

On étudie brièvement l'emploi des coefficients tabulés aux problèmes sur les corps antiferromagnétiques.

Die ersten sechs Koeffizienten in der Entwicklung der Suszeptibilität χ, und ihrer Reziproken χ^{-1} nach steigenden Potenzen der reziproken Temperatur werden nach der Heisenbergschen Theorie des Ferromagnetismus für beliebige Werte des Spins S und beliebige Kristallgitter berechnet. Die ersten fünf Koeffizienten in der Entwicklung der magnetischen spezifischen Wärme C werden ebenfalls bestimmt. Die Koeffizienten von χ und C für raumzentrierte und flächenzentrierte kubische Gitter werden für die Spinwerte von $\frac{1}{2}$ bis 3 tabelliert.

Mit Hilfe dieser Koeffizienten wird die reduzierte Curie-Temperatur $\theta_c=kT_c/J$ abgeschätzt. Man findet, dass für einfache, raum- und flächenzentrierte kubische Gitter die Formel

$$\theta_c=\tfrac{5}{96}(z-1)(11X-1)$$

die geschätzte Curie-Temperatur ziemlich genau wiedergibt. Hier ist $X=S(S+1)$ und z bedeutet die Koordinationszahl des Gitters.

Man findet, dass bei geeigneter Änderung des Masstabes die theoretischen Kurven der reziproken Suszeptibilität als Funktion der Temperatur oberhalb des Curie-Punkts vom Betrag des Spins und von der genauen Gitterstruktur nur wenig beeinflusst werden. Das Verhältnis des anfänglichen zum asymptotischen Gradienten beträgt ungefähr 0,3. Die berechneten und experimentellen Werte von χ^{-1} werden für Eisen und für Nickel verglichen. Wenn man Eisen durch ein Heisenbergsches Modell mit $S=1$ darstellt, so entspricht die beobachtete Curie-Temperatur einem Wert von J gleich $1{,}19\times10^{-2}$ ev.

Die Verwendbarkeit der tabellierten Koeffizienten für antiferromagnetische Probleme wird kurz besprochen.

References

[1] Opechowski, W., 1937, *Physica*, **4**, 181.
[2] Opechowski, W., 1938, *Physica*, **6**, 1112.
[3] Zehler, V., 1950, *Z. Naturf.*, **5a**, 344.
[4] Brown, H. A., and Luttinger, J. M., 1955, *Phys. Rev.*, **100**, 685.
[5] Brown, H. A., 1956, *Phys. Rev.*, **104**, 624.
[6] Rushbrooke, G. S., and Wood, P. J., 1955, *Proc. phys. Soc. Lond.* A, **68**, 1161.
[7] Domb, C., and Sykes, M. F., 1956, *Proc. phys. Soc. Lond.* B, **69**, 486.
[8] Wood, P. J., and Rushbrooke, G. S., 1957, *Proc. phys. Soc. Lond.* A, **70**, 765.
[9] Danielian, A., and Stevens, K. W. H., 1957, *Proc. phys. Soc. Lond.* B, **70**, 326.
[10] Domb, C., and Sykes, M. F., 1957, *Phil. Mag.*, **2**, 733.
[11] Domb, C., and Sykes, M. F., 1957, *Proc. phys. Soc. Lond.* B, **70**, 896.
[12] Kasteleijn, P. W., and van Kranendonk, J., 1956, *Physica*, **22**, 317.
[13] Frank, D., 1956, *Z. Phys.*, **146**, 615.
[14] Domb, C., and Sykes, M. F., 1957, *Proc. roy. Soc.* A, **240**, 214.
[15] Sucksmith, W., and Pearce, R. R., 1938, *Proc. roy. Soc.* A, **167**, 189.
[16] Néel, L., 1934, *J. Phys. Rad.*, **5**, 104.
[17] Stoner, E. C., 1946–7, *Reports Progr. Phys.*, **11**, 43.
[18] Griffith, J. S., 1956, *J. Inorg. nucl. Chem.*, **3**, 15.
[19] Mott, N. F., and Stevens, K. W. H., 1957, *Phil. Mag.*, **2**, 1364.